How was the MRI model applied?

Kathleen F. Jones

Cold Regions Research and Engineering Laboratory, Hanover, New Hampshire, U.S.A.

kathleen.f.jones@usace.army.mil

Abstract— **Meteorology Research Incorporated (MRI) undertook icing studies for numerous utilities in North America in the 1970s, 1980s, and 1990s using their icing model for freezing rain, supercooled clouds, wet snow, and vapor deposition. MRI's reports to Ontario Hydro and Bonneville Power Administration include assumed parameter values and source code, as well as output for modeled storms in Michigan and Washington for which I had also acquired weather data for icing studies. In this paper I recreate the MRI analyses of freezing rain storms in Michigan to understand how their ice loads were determined. I use this model to examine the effects of eliminating hoar frost or rime icing or wet snow accretion on glaze ice loads in a freezing rain event. For the cases in Washington, intended to simulate in cloud icing at higher elevations, I suggest more realistic choices for the properties of supercooled clouds in the absence of site data.**

Keywords— ***MRI model, ice load, transmission line, ice density, in cloud icing, wet snow, hoar frost***

I. Introduction

From the 1970s through the early 1990s Meteorological Research Incorporated (MRI), followed by Richmond Meteorological Consulting, carried out icing studies for utilities and consulting engineers for a utility's service area or for existing or proposed transmission lines in the United States and Canada. These studies were done for Southern California Edison, Pacific Power and Light, Hydro Quebec, Calgary Power, British Columbia Hydro, Montana Power, Newfoundland and Labrador Hydro, Ontario Hydro, Bonneville Power Administration, San Diego Gas and Electric, Platte River Power Authority, Toledo Edison, and proposed transmission line routes in Alaska (personal communication, M.C. Richmond, 1993).

The MRI model for ice loads from freezing rain includes a heat balance calculation and assumes that any impinging water that does not freeze drips off, without allowing for the formation of icicles. Therefore, one might expect these MRI modeled ice loads to be relatively small. However, my impression from discussions with utility engineers over the years is that MRI loads for lines in their service area are substantially higher than loads I calculate using the Simple model [1] that assumes all impinging freezing rain freezes to the conductor. I speculated that the large ice loads that MRI had determined were obtained by decreasing the assumed fall speed of the rain drops, which increases the liquid water content in the air and therefore the wind blown flux of rain drops. For this paper, I studied the MRI model, including its snow accretion and in cloud icing algorithms and assumptions as well as its freezing rain formulation, to determine how it works. I used the report MRI wrote for Ontario Hydro [2] that Dr. Samy Krishnasamy had given me a copy of when he was an engineer at Ontario Hydro as well the MRI report to BPA [3] that Dr. Alan Peabody provided. The Ontario Hydro report includes MRI model output from an icing storm in March 1976 that hit both Flint and Saginaw, Michigan. The BPA report includes MRI model output for four icing events in 1949 and 1950 at Spokane, Washington. Both reports include a listing of the source code for the version of the MRI model that was used.

In the next section I present and discuss the freezing rain, wet snow, in cloud, and vapor icing algorithms included in the MRI model. That is followed by the Saginaw and Flint results from my application of the MRI model and a discussion of the implications of some of the MRI assumptions. I also compare the MRI weather data at those locations with the weather data archived by the National Centers for Enviromental Information (NCEI) and run the Simple model augmented by a model for ice accretion in fog and an internally consistent version of MRI's wet snow model. In the following section I present and discuss the MRI simulations at Spokane that are focused on in cloud icing at higher elevations.

II. MRI model

The MRI model as applied in [2] has four possible sources for accretion on conductors and ground wires: hoar frost from vapor, rime from supercooled clouds, glaze from freezing rain, and snow from wet snow. In any hour, a combination of these loads may be applied. Flags that were set in a previous step of the MRI process specify which of these accretions occur in each hour. In the following I describe each of the algorithms for each icing type from the source code listing in Appendix A of [2].

A. Freezing Rain

The assumed precipitation drop diameter in freezing rain d_Z = 2000 µm, which is used to determine the collision efficiency of the rain drops with the conductor. For the Saginaw simulation the fall speed for the rains drops u_f = 4.09 m/s is specified, however the default value in the Fortran program is 4.03 m/s. The total drop speed, used in the collision efficiency calculation and the flux of water to the conductor, is the vector sum of u_f and the wind speed u. The incremental mass of glaze ice per unit length accreted in time step $\Delta\tau$ is

$$\Delta m_z = E\left[d_z, u_{tot}, D_i\right] u_{tot} D_i \frac{P \rho_w}{u_f} \Delta\tau \qquad (1)$$

where

P: precipitation rate
ρ_w: density of water = 1 g/cm^3
$D_i = D_0 + 2t_i$: iced conductor diameter
D_0: bare conductor diameter
t_i: radial thickness of ice accretion
$u_{tot} = (u^2 + u_f^2)^{1/2}$: total drop speed
$E[d_z, u_{tot}, D_i]$: collision efficiency of drops with conductor.

B. Wet Snow

The formulation for the accretion of wet snow is similar to the freezing rain formulation. The sticking fraction S of the snowflakes with the conductor is set to 0.25. The diameter of the snow flake

$$d_s\left[\mu\text{m}\right] = 1940P^{0.48} \qquad (2)$$

is used to calculate the collision efficiency with the conductor. The incremental mass of snow per unit length accreted in time step $\Delta\tau$ is

$$\Delta m_s = E\left[d_s, u_{tot}, D_i\right] S u_{tot} D_i W_s \Delta\tau \qquad (3)$$

Where W_s=0.223$P^{0.85}$ is the liquid water content of the snow filled air. Note that the assumed fall speed of the precipitation, used in computing u_{tot} for both freezing rain and snow, is inconsistent with the liquid water content W_s determined from the precipitation rate.

C. Supercooled fog

In hours with icing from supercooled clouds or fog, the MRI model assumes a cloud drop diameter d_c=40 μm and liquid water content W=0.5 g/m^3. The incremental mass of rime ice per unit length accreted in time step $\Delta\tau$ is

$$\Delta m_c = E\left[d_c, u, D_i\right] u D_i W \Delta\tau\,. \qquad (4)$$

The tentative total ice mass increment in a time step is the sum $\Delta m_{tot}=\Delta m_z+\Delta m_s+\Delta m_c$. If the accretion includes wet snow, it is considered dry. Otherwise a subsequent calculation determines how much ice Δm_{test} could accrete. If $\Delta m_{tot} < \Delta m_{test}$, the accretion is considered dry. If not, the accretion is wet and Δm_{tot} is set to $\Delta m_{test.}$

D. Vapor

If the accretion is determined to be dry, the MRI model allows ice to accrete from the vapor phase, apparently assuming a relative humidity of 98%. The formulation for determining the mass of hoar frost in the MRI model references [4]. I did not include a calculation of hoar frost mass in my version of the MRI model, and instead used the hourly masses of accreted hoar frost from [2].

E. Process

The MRI model divides each hour into six time steps ($\Delta\tau$=10 minutes), with the weather parameter values in the i^{th} step interpolated from the values in the previous hour j-1 and this hour j:

$$x_{j,i} = \frac{(6-i)}{6} x_{j-1} + \frac{i}{6} x_j\,, \qquad (5)$$

where x is air temperature, wind speed, or precipitation rate. At the 6$^{\text{th}}$ time step the parameter values are the values for the jth hour. For each hour there are four icing type flags, with each set to 0 (no ice accretion) or 1 (ice accretion). For each time step, the icing type flags are set to the maximum value. That means that any icing type persists for at least two hours. The densities of these accretions are:

- Glaze ice ρ_z=0.9 g/cm^3
- Wet snow ρ_s=0.5 g/cm^3
- Rime ice ρ_c=0.4 g/cm^3, according to the list of parameters for the Saginaw analysis and in the default value in the MRI source code, but the text specifies a rime density of 0.6 g/cm^3
- Hoarfrost ρ_v=0.1 g/cm^3.

At the end of each time step, the average mass-weighted ice density ρ_i is computed for Δm_{tot} and the incremental volume of ice $\Delta V = \Delta m_{tot} / \rho_i$ is spread uniformly thickly over the ice-covered conductor diameter from the previous time step. At the end of each hour, the incremental ice mass for each accretion type, total incremental ice mass, ice thickness t_i, ice-covered conductor diameter, and total ice mass are output, along with the wind speed, air temperature, and rainfall rate.

The results of the application of my formulation of the MRI model for a storm in March 1976 at Saginaw and Flint, Michigan, are presented in the next section along with a comparison of the MRI weather data with archived data.

III. Michigan Storm, March 1976

In early March 1976 a freezing rain storm hit both Saginaw and Flint, Michigan. Refernce [2] shows weather data along with ice loads and ice thicknesses computed by the MRI model in Table IX-2 for Saginaw and IX-3 for Flint. MRI uses metric units in their program but converts output to English units. I converted the values of wind speed (miles/hr), rainfall rate (inches in 6 hours), ice load (pounds/ft), and iced conductor diameter (inches) to metric units (m/s, mm/hr, g/cm, and cm, respectively) for this analysis. I wrote a Fortran program to execute the MRI model with the ice accretion formulations in Section II. I also copied the MRI subroutine for collision efficiency, correcting a line of code that uses an undefined CX to use the intended DX instead. As a first check on my code, I used the modeled incremental ice loads from Tables IX-2 and 3 in each hour to calculate the new iced diameter for that hour. This calculated diameter time series agreed perfectly with the values in the report.

The real test, however, requires calculating for each hour the incremental ice mass of each accretion type. For both simulations, I found that my computed hourly ice masses were slightly larger than the values in the report, as shown in Figure 1 for the freezing rain and supercooled fog at Saginaw. I initially attributed this to the uncertainty in MRI's collision efficiency code with the CX typo. However, that error is not in [3] and I have the same slightly too high ice loads for those cases. To better match the MRI final ice masses, I include a multiplicative factor in the mass calculation for glaze, rime, and snow that I adjusted by trial and error. The adjustment factors are different for Flint and Saginaw, and are different for the different icing modes.

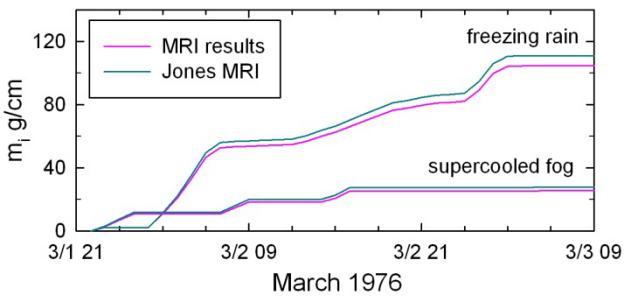

Fig. 1. Comparison of the MRI model results for freezing rain and supercooled fog at Saginaw with the formulation of that model in this paper attempting to reproduce those results.

A. Saginaw

The MRI model results in [2] are for ice accreted on a 2.54-cm diameter conductor. My correction factors are 0.973 for freezing rain and 0.973^3=0.921 for fog. Time series of the output from running my version of the MRI model with the correction factors are shown in Figure 2. Figure 2a shows the total ice mass and the mass for each icing type, 2b shows the density of ice, along with the accretion types, in each hour, and 2c is the total ice thickness. The final ice mass and ice thickness are 136.5 g/cm and 6.7 cm, compared to 136.5 g/cm and 6.3 cm in [2]. The contributions to the total ice load from freezing rain, supercooled fog, and vapor deposition are shown in the first line of Table 1. The average ice density of 0.77 g/cm^3 is low enough that the accreted ice would look white, in contrast to typical ice accretions from freezing rain that are clear with some air bubbles.

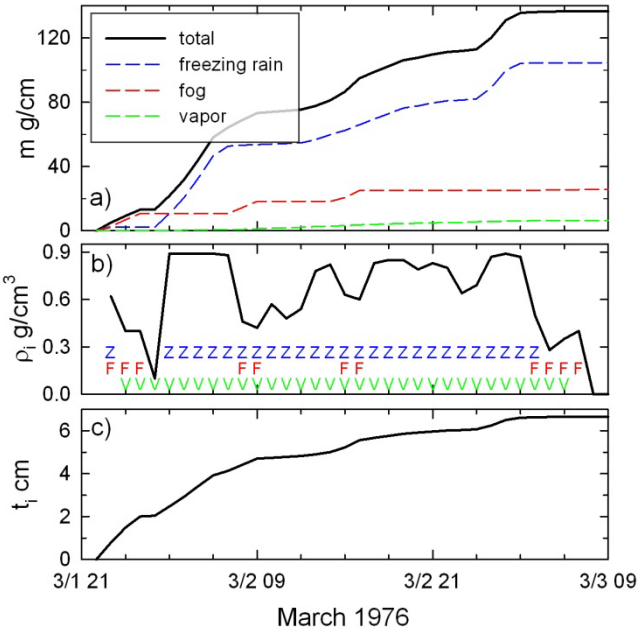

Fig. 2. Ice accretion simulation for Saginaw implementing the MRI model: a) ice load, showing the load for each icing type as well as the total, b) icing type in each hour (Z=freezing rain, F=fog, V=vapor) and the density of the accreted ice, and c) accreted ice thickness.

In subsequent simulations, I reran the Saginaw data without including the deposition of ice from vapor, then without accreting ice from supercooled fog, then without either. Table 1 compares these results to the original simulation with all three ice types included and shows the significant effect of the iced diameter on the mass of subsequent increments of glaze ice. Although the thickness of the glaze increments is not affected by these previous accretions (the calculated collision efficiency is close to 1), the incremental mass of a layer farther from the center of the conductor is larger. Excluding rime ice accretions from supercooled fog, with the assumed large drop size and liquid water content and low density, not only removes 25.6 g/cm of rime ice, it also removes 35 g/cm of glaze ice, reducing the total ice load by 44% and the ice thickness by 34%. Excluding the deposition of ice from the vapor phase has a smaller effect, removing 3.5 g/cm of glaze ice in addition to the 6.5 g/cm of hoarfrost. The simulation that excludes deposition from the vapor (the air was not saturated) and rime from high liquid water content fog (visibilities were relatively high) is more realistic than the MRI simulation. The accreted ice mass and ice thickness for that simulation are 45% and 54%, respectively, of the MRI results.

It is also worthwhile to compare the weather data MRI used with the archived weather data. At the time MRI did the icing study for Ontario Hydro, weather data was available for stations in the United States from the National Climatic Center on 9-track magnetic tape. Hourly weather data is now available from ISD (Integrated Surface Database ftp://ftp.ncdc.noaa.gov/pub/data/noaa) and daily precipitation data is archived in the GHCN (Global Historical Climatology Network ftp://ftp.ncdc.noaa.gov/pub/data/ghcn/daily/) database. The daily precipitation data measured using manual gauges at the COOP (Cooperative Observer Program) stations collocated with first-order weather stations is considered better than the hourly, 6-hourly, or 24-hourly precipitation data from the automatic gauges at the first-order stations (Neal Lott, personal communication and https://www.cocorahs.org/Content.aspx?page=faqgeneral#autogauges). I prorate that accumulated daily precipitation to each hour using the present weather codes for the hours and the table of weighting factors in [5] that is based on a table provided by Tsoi Yip (unpublished) that she used to prorate 24-hr precipitation amounts for an ice load map of Canada. I used the visibility V in each hour with fog to estimate the liquid water content of the fog, using the MRI assumed cloud drop diameter of 40 μm and the relation between V and W from [6]

$$W\left[\mathrm{g/m^3}\right] = \frac{\rho_w\left[\mathrm{g/cm^3}\right] d_c\left[\mu\mathrm{m}\right]}{V\left[m\right]} \qquad (6)$$

This equation is derived from the relationship in [7] between liquid water content, drop diameter, and extinction coefficient and the relation in [8] between daytime visual range at a threshold contrast of 2% and extinction coefficient. Note that a larger assumed drop diameter results in a larger

Table 1. Ice masses, average ice density, and total ice thickness for Saginaw, for the original MRI simulation and for versions without ice from vapor and/or fog.

	glaze g/cm	rime g/cm	hoar frost g/cm	total g/cm	Ice density g/cm^3	ice thickness cm
Freezing rain, rime ice, and hoarfrost	104.4	25.6	6.5	136.5	0.77	6.7
No hoarfrost	100.9	25.6	0	126.5	0.80	6.2
No rime ice	69.4	0	6.5	75.9	0.83	4.4
Freezing rain only	61.9	0	0	61.9	0.90	3.6

liquid water content, which results in a larger ice load from the higher collision efficiency and the larger flux of cloud water.

The MRI weather data and the processed ISD and COOP weather data for Saginaw are compared in Figure 3. The air temperatures in Fig. 3a are generally in agreement, and where they are not, early on 2 March, the differences do not matter. MRI did not use dew-point temperature T_d, which may be why they deposited ice from vapor in hours when the air was not saturated, assuming a relative humidity of 98%. The big swings in the ISD T_d between 09:00 and 16:00 may be attributable to the difficulties in making that measurement when it is cold and wet. The MRI and ISD wind speeds in Fig. 3b agree well, with minor differences in only two hours. There are significant differences, however, in the hourly precipitation in Fig. 3c. MRI hourly precipitations are apparently based on 6-hourly accumulations. That, however, does not explain their much higher total precipitation compared to the COOP data. Fig. 3d shows the CRREL fog liquid water content calculated from the ISD visibility and the assumed MRI d_c=40 µm. MRI values of 0.5 g/m^3 tend to coincide with hours when the calculated W is 0.01 g/m^3 or higher. This panel also shows the precipitation type in each hour from [2] (black) and present weather reported in the ISD data (red). I treat all the precipitation in any hour with freezing rain, and possibly other precipitation types, as all freezing rain, indicated by Z. Hours with ice pellets are indicated by I, and rain by R. I treat rain at a temperature below freezing as freezing rain. I run the CRREL and Simple models in two modes; one in which ice accretes only in hours with freezing rain, and another in which ice accretes in hours with ice pellets as well, assuming that there may be areas near the weather station where that precipitation is falling as freezing rain.

I ran an augmented Simple model using this processed ISD and COOP data as input. My addition to the Simple model calculates W from visibility with d_c=40 µm and accretes ice from supercooled fog, using the Finstad collision efficiency formulation [9]. It also accretes wet snow, using an internally consistent formulation of the MRI snow accretion model. Collision efficiency is not calculated for precipitation drops because they are falling and the commonly used collision efficiency calculation applies only to drops that are small enough that they move only when carried by the wind. In hours with freezing rain, all the ice that accretes from any source is assumed to be glaze ice with a density of 0.9 g/cm^3. For the case in which ice pellets are treated as freezing rain, consistent with the MRI approach, the total ice load is 48.2 g/cm and the ice thickness is 3.1 cm, 78% and 86%, respectively, of the freezing-rain-only case in Table 1. The difference is due to primarily to the smaller precipitation amounts in the COOP data compared to the MRI values.

B. Flint

The March 1976 storm that hit Saginaw with freezing rain was snow and freezing rain in Flint, 58 km to the south. MRI modeled the accretion of ice from freezing rain, wet snow, supercooled fog, and vapor on a 2.54-cm diameter conductor. Correction factors of 0.988 for in cloud icing and 0.964=0.988^2, for freezing rain and wet snow in my version of the MRI model provided the best agreement with the MRI ice loads and thicknesses at Flint. With these factors, the ice thickness is 4.1 cm and the ice load is 48.3 g/cm compared to 4.0 cm and 48.4 g/cm obtained by MRI. The time series of my implementation of the MRI model for Flint in Figure 4 shows that supercooled fog is the largest contributor to accreted ice load, followed by freezing rain and wet snow.

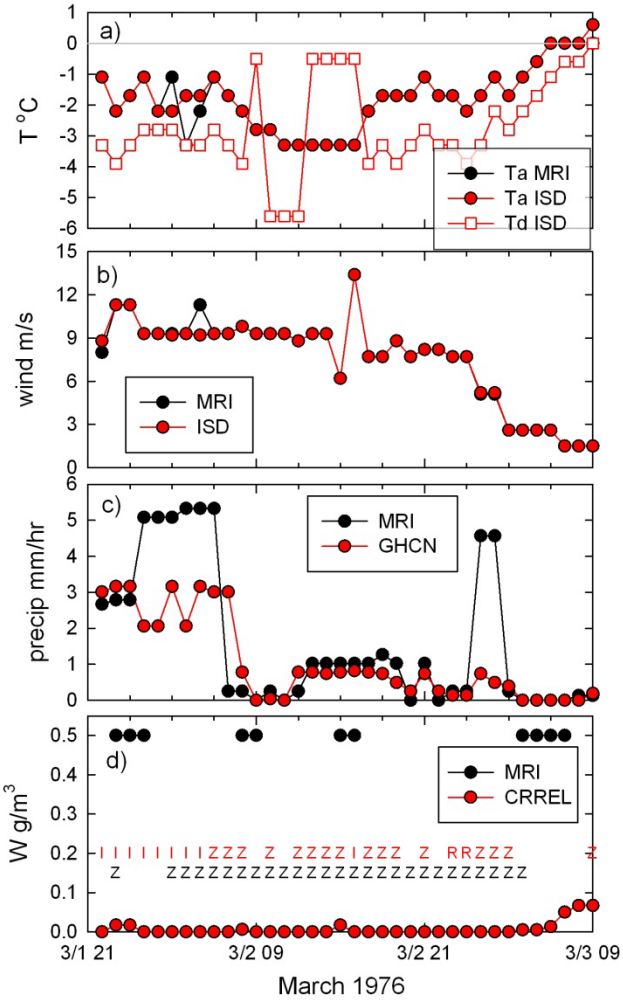

Fig. 3. Comparison of Saginaw weather data from MRI with weather data based on ISD and GHCN a) air T_a and dew-point temperature T_d, b) wind speed, c) hourly precipitation, and d) liquid water content of fog, and precipitation type (Z=freezing rain, I=ice pellets, R=rain).

As for Saginaw, I examine the effect of each of the non-freezing rain contributions to the total ice load (Table 2). The wet snow at Flint adds an additional complication. In hours with both freezing rain and snow, MRI uses the precipitation in that hour to generate the glaze ice load and then reuses that precipitation to compute the wet snow load. Not allowing wet snow to accrete in hours with freezing rain reduces the glaze ice load because of the smaller iced diameter, in addition to significantly reducing the accreted snow load. Turning off the accretion of ice from the vapor phase and from supercooled fog for the same reasons as at Saginaw (the air is not saturated and visibilities are relatively high) reduces the glaze ice load because of the reduction in iced diameter, but the biggest effect is the loss of the rime ice load which is half of the total. Accreting only ice from freezing rain and wet snow in hours without freezing rain

reduces the total ice load to 24% of the MRI value and the ice thickness to 29% of the MRI value. This more realistic simulation changes the appearance of the accretion from MRI's rough white ice to smooth, nearly clear glaze ice.

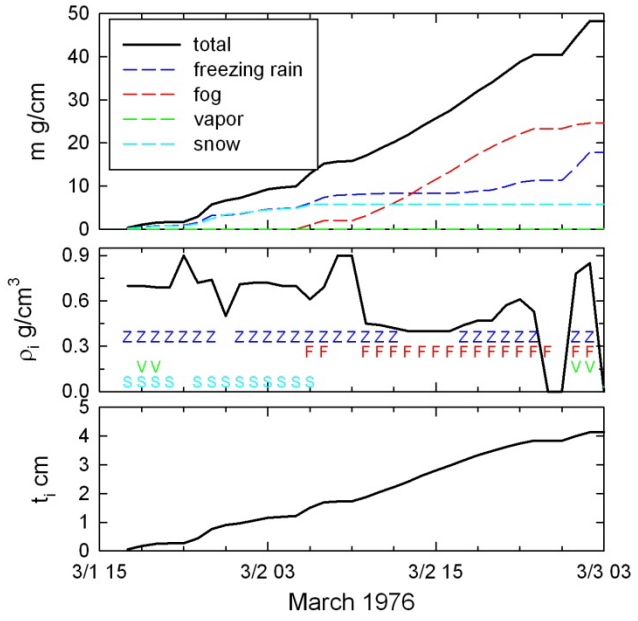

Fig. 4. Ice accretion simulation for Flint implementing the MRI model: a) ice load, showing the load for each icing type as well as the total, b) icing type in each hour (Z=freezing rain, F=fog, V=vapor, S=wet snow) and the density of the accreted ice, and c) accreted ice thickness.

The MRI weather data and my processed ISD and GHCN weather data for Flint are compared in Figure 5. What is immediately obvious is the big difference in air temperatures in Fig. 5a. MRI apparently changed 26 hours of reported above-freezing temperatures to -0.6°C, possibly justified by the observations of freezing rain in many of those hours. Dew-point temperatures are quite low that entire time. MRI wind speeds agree well with ISD wind speeds in Fig 5b. MRI hourly precipitation rates in Fig. 5c show relatively good agreement with the daily precipitation amounts prorated to each hour. However, the MRI total precipitation for this time period is greater than the archived COOP amounts. MRI accumulated rime ice for many hours at Flint (Fig. 5d) when visibilities were relatively high, as shown by the small calculated *W*. It is greater than 0.01 g/m^3 in only four hours. Running the augmented Simple model for Flint using the ISD data results in a total ice load of 7.8 g/cm and an ice thickness of 0.8 cm, significantly smaller than the most realistic MRI values shown in the bottom line of Table 2. The difference is due primarily to the fewer hours with freezing rain in the ISD data and the smaller precipitation amounts in the COOP data compared to the MRI values.

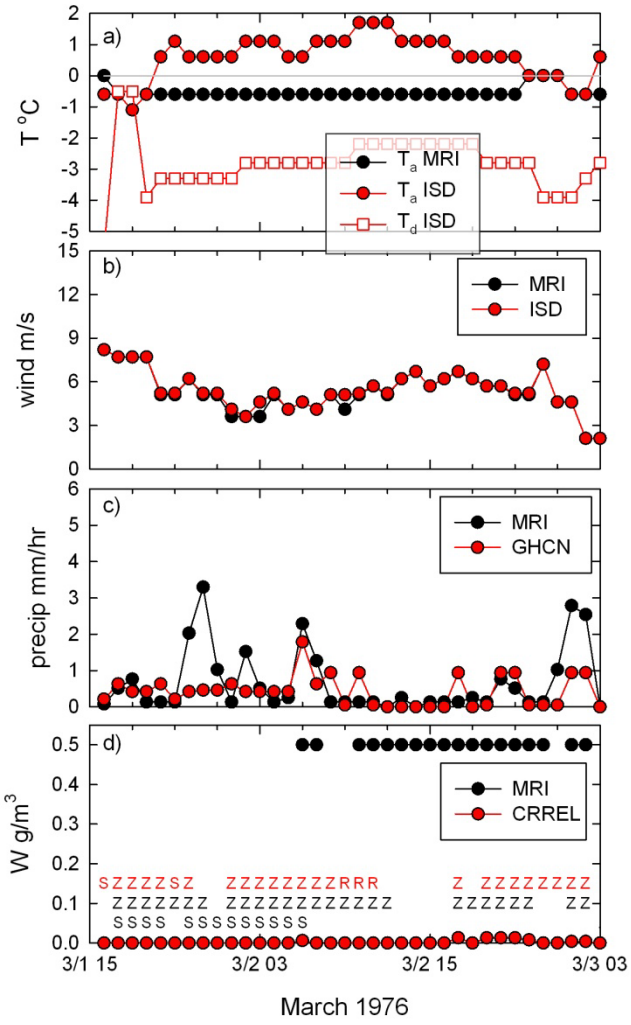

Fig. 5. Comparison of Flint weather data from MRI with weather data based on ISD and GHCN a) air T_a and dew point temperature T_d, b) wind speed, c) hourly precipitation, and d) cloud liquid water content and precipitation type (Z=freezing rain, S=snow, R=rain).

In the next section I discuss the MRI model results at Spokane, Washington, that are included in [3]. The Spokane events are different from the Michigan events in that the temperature and wind data at Spokane is adjusted apparently

Table 2. Ice loads, average ice density, and total ice thickness for Flint, for the original MRI simulation and for variations that exclude specific accretion modes, ultimately including only freezing rain and some wet snow.

	glaze g/cm	snow g/cm	rime g/cm	hoar g/cm	total g/cm	Ice density g/cm3	ice thickness cm
Freezing rain, rime ice, wet snow and hoarfrost	17.9	5.8	24.6	0.1	48.3	0.60	4.1
Wet snow only in hours without freezing rain	15.7	0.8	24.6	0.1	41.1	0.59	3.8
No hoar or rime	13.6	5.7	0	0	19.3	0.78	1.8
Freezing rain and wet snow in hours without freezing rain	10.8	0.7	0	0	11.5	0.88	1.2

to simulate ice accreting at higher elevations in supercooled fog.

IV. Spokane

Reference [3] uses the MRI model to determine ice loads at weather stations and, by extrapolation, at sites near weather stations in the Pacific Northwest region of the United States, covering the BPA service area. MRI acquired weather data on magnetic tape for 42 stations in the states of Washington, Oregon, Idaho, and Montana from 1948 to 1964. They simulated the accretion of ice from vapor, supercooled fog, wet snow, and freezing rain on a 1.3-inch (30.5-mm) diameter conductor. Their simulations differ from those for Ontario Hydro, using a rime ice density of 0.6 g/cm^3 and a rain drop fall speed of 4.03 m/s. The only model results at a weather station that are included in the report are in sub-Appendix C with no accompanying explanation. The headers of these four events, indicate that they are all for Spokane, Washington.

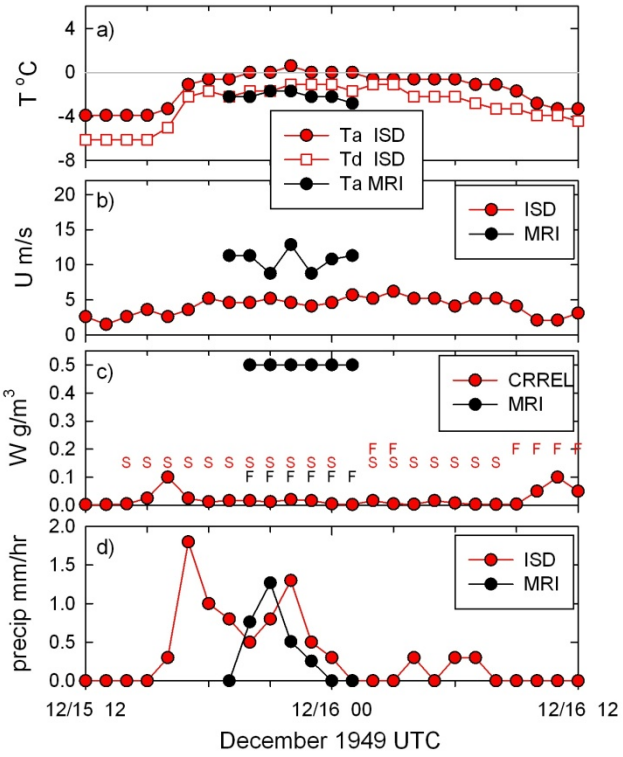

Fig. 6. MRI and ISD weather data for Spokane for the December 1949 supercooled fog event.

Time series of the MRI weather data including hourly precip amounts, is shown in Figure 6 for the event in December 1949, along with the ISD data for that day. The other MRI input data at Spokane are similar, with colder temperatures and higher winds than the ISD data, while the MRI precipitation is comparable to the archived amounts. The dominant source of the accreted ice load in all four events is the assumed W=0.5 g/m^3 and d_c = 40 μm in the supercooled fog. The two MRI events in 1949 accrete ice only from supercooled fog. The November 1950 MRI event includes two hours of wet snow but 95% of the ice load is from supercooled fog. The December 1950 MRI event has 9 hours of simultaneous freezing rain and supercooled fog, with 84% of the accreted load from supercooled fog. To evaluate this sample of MRI loads based on the Spokane weather data, but at some higher elevation, with no visibility data or other source of information on the local fog properties, we need to examine the MRI assumptions.

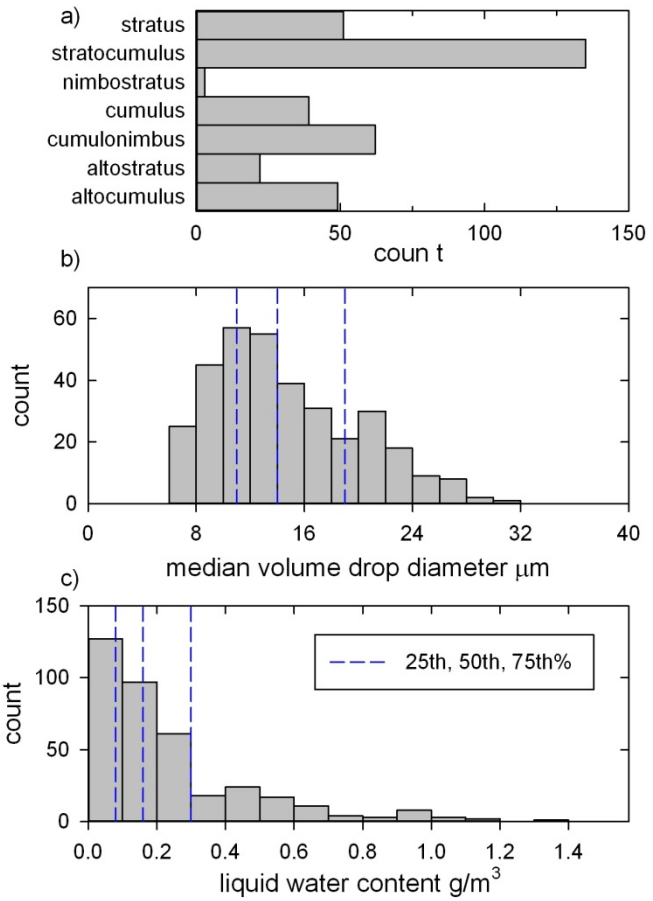

Fig. 7 Properties of supercooled clouds from the Jeck database a) cloud type, b) drop diameter, and c) liquid water content. The dashed blue lines in (b) and (c) indicate the 25th, 50th, and 75th% values.

I used Jeck's database of measured properties of clouds (personal communication, Richard Jeck) over Alberta, British Columbia, Montana, Idaho, and Washington to provide realistic values of cloud liquid water content and median volume drop diameter for clouds over elevated terrain near Spokane. See [10] for a complete compilation of cloud property measurements from flights in supercooled clouds. Figure 7 shows histograms of cloud type and properties for ~350 flights in supercooled clouds. The most common cloud type for these measurements is stratocumulus, followed by cumulonimbus and stratus. The 25th, 50th, and 75th percentile drop diameters are substantially smaller than the 40 μm assumed by MRI; the largest diameter is 32 μm. The 25th, 50th, and 75th% liquid water contents are all smaller than MRI's 0.5 g/m^3, which is greater than 87% of the measured values. To be conservative but still realistic, we could assume that clouds at the higher elevations near Spokane have the 75th% Jeck properties, d_c=19 μm and W=0.30 g/m^3.

I specified these cloud properties in my version of the MRI model along with the MRI weather data to estimate ice

loads for three of the Spokane events. They are compared with the MRI loads in Table 3. The November 1950 event is not modeled because that accretion was wet and I did not include MRI's heat balance calculation in my version of the model. The much smaller ice loads with these more realistic cloud properties is due in part to the reduced cloud liquid water content, but is primarily caused by the much smaller collision efficiencies of the 75th% Jeck cloud drops, with a mass that is only 11% of the mass of the MRI cloud drops.

One could also estimate reasonable drop diameters using the relationship in [11] that relates drop diameter to wind speed and air temperature

$$d_c = -0.63 + \frac{24.56}{\sqrt{u}} + 12.418 e^{T_a/19.9} \qquad (7)$$

using the averages of the extrapolated wind speeds and temperatures for each of the events. The resulting drop diameters for the four events chronologically are 17, 18, 19, and 23 μm. Only the Dec 1950 drop size is larger than the 75th % value from the Jeck data, and results in a 2.5 g/cm ice load.

Table 3. Comparison of ice loads at Spokane for the original MRI cloud properties and for conservative, yet reasonable cloud properties based on the Jeck database of measurements in clouds over the Pacific Northwest and adjacent Canadian provinces.

Spokane in cloud icing event	MRI ice load g/cm	Jeck 75th% clouds ice load g/cm
Feb 1949	12.1	2.8
Dec 1949	25.9	4.8
Nov 1950	20.1	-
Dec 1950	8.5	1.9

V. Summary and Conclusions

This analysis of the application of the MRI icing model points out a number of ways in which the model as applied with the assumed parameter values is excessively conservative. MRI assumes a 98% relative humidity in hours with freezing rain, even though the difference between the air temperature and dew-point temperatures indicates much lower relative humidities. MRI's deposition of hoar frost from the vapor phase at a density of 0.1 g/cm^3 increases the ice load from freezing rain because that ice is accreted on a larger iced diameter. That effect is even greater when rime ice is accreted in freezing rain events. The assumed supercooled fog properties are unrealistically conservative. Together with the assumed rime density of 0.4 or 0.6 g/cm^3, these assumptions result in significant rime ice accretions as well as greatly increased accretions from freezing rain in the subsequent hours because of the larger iced diameter. Wet snow accreted at 0.5 g/cm^3 has a similar effect, but its primary excess in the MRI model is that the precipitation in hours with both freezing rain and snow is used to compute the glaze ice mass increment and then used again to compute the wet snow increment. I did not investigate the effect of the internal inconsistency in the wet snow model, but it is probably minor compared to these other issues. Finally, the MRI precipitation amounts, in the cases available for examination, are significantly larger than the archived values. That also generates excess ice loads.

Acknowledgment

I thank Ronald Thorkildson and Alan Peabody for useful conversations about the MRI model applications.

References

[1] Jones, KF, 1996. A simple model for freezing rain ice loads. *Proceedings of the 7th International Workshop on Atmospheric Icing of Structures*, Chicoutimi, Canada, 412–416.

[2] Anderson, RS and MC Richmond, 1977. Ontario-Hydro wind and ice loading model, MRI 77 FR-1496, May 1977.

[3] Richmond, MC, SC Gouze, and RS Anderson, 1977. Pacific Northwest icing study, MRI 77 FR-1515, September 1977.

[4] Cotton, WR, 1970. A numerical simulation of precipitation development in supercooled cumuli, Penn State University, Report No. 17 to National Science Foundation, NSF GA-13818.

[5] Jones, KF, 2003. Ice storms in the St. Lawrence Valley region, ERDC/CRREL TR-03-1, Cold Regions Research and Engineering Laboratory, Hanover, New Hampshire.

[6] Jones, KF and G Koh, 1995. The rotating multicylinder, *Proceedings of the 4th Annual Mt. Washington Observatory Symposium*, June 1995, Gorham, New Hampshire, 35-43.

[7] Winstanley, JV and MJ Adams, 1975. Point visibility meter: a forward scatter instrument for the measurement of aerosol extinction coefficient, *Applied Optics*, 14, 2151-2157.

[8] Kumai, M, 1973. Arctic fog droplet size distribution and its effect on light attenuation, *J. Atmospheric Sciences*, 30, 635-643.

[9] Finstad, KF, EP Lozowski, and EM Gates, 1988. A computational investigation of water droplet trajectories, **5**, 160-170.

[10] Jeck, RK, 2008, Advances in the characterization of supercooled clouds for aircraft icing applications, DOT/FAA/AR-07/4, U.S. Dept. of Transportation, Federal Aviation Administration.

[11] Jones, KF, RM Thorkildson, and JB Eylander, 2017. Median volume drop diameter for in cloud icing simulations, *Proceedings of the 17th International Workshop on Atmospheric Icing of Structures*, Chongqing, China, paper B2-3.